DOI: 10.35595/2414-9179-2024-1-30-507-533

Maretta L. Kazaryan[1], **Mikhail A. Shahramanian**[2,3], **Vladimir S. Tikunov**[4], **Irina N. Tikunova**[5]

APPLICATION OF DISCRETE ORTHOGONAL TRANSFORMATIONS FOR IDENTIFYING AND DISPLAYING MUNICIPAL SOLID WASTE IN GEOINFORMATION SYSTEMS ON THE EARTH'S SURFACE

ABSTRACT

Space monitoring in conditions of increased risk of emergencies of a natural and man-made nature and the involvement of medical and preventive measures to maintain the health of the population (flora, fauna) in critical situations is an urgent task. The method of digital spectral transformations is widely used in a variety of applied problems. In particular, when processing space information, it is advisable to use them. Cosmic information, in general, in mathematical representation, is a multidimensional variety. When working with ordinary images we have a two-dimensional manifold, when working with stereo images we have three-dimensional manifolds, when working with a series of stereo images (time series) we have four-dimensional manifolds. The mathematical basis for determining anomalous signal structures in the surrounding background is the concept of continuous orthogonal transformations; in this work we will specifically consider the Fibonacci transformations. The paper examines the problem of optimal zone coding using a discrete Fibonacci transform and analyzes the main properties of this transform, derives estimates of the spectrum of a discrete Fibonacci transform on a class of Lipchitz signals and clarifies the form of the selection matrix S when performing compression through zone coding using a discrete Fibonacci transform. An experiment is presented to identify unauthorized solid waste on the Earth's surface using research conducted on the basis of discrete orthogonal transformations.

KEYWORDS: compression of the signal, space monitoring, remote sensing of the Earth, emergency situations, medical and preventive measures, discrete orthogonal transformations

INTRODUCTION

The paper discusses a mathematical approach in research devoted to space monitoring and analysis of satellite images [*Kazaryan*, 2021].

One of the quantitative characteristics of any image is the spectral brightness of its elements. It is this characteristic that is fundamental when performing image recognition and identifying changes in certain areas of the Earth using satellite images [*Crippen*, 1990; *Garcia* et al., 2006; *Schowengerdt*, 2013].

[1] North Ossetian State Medical Academy of the Ministry of Health of the Russian Federation, 40, Pushkinskaya str., Vladikavkaz, Republic of North Ossetia — Alania, 362019, Russia, *e-mail:* **marettak@bk.ru**

[2] SSI "Institute for Scientific Research of Aerospace Monitoring 'AEROCOSMOS'", 4, Gorokhovsky ln., Moscow, 105064, Russia, *e-mail:* **7283763@mail.ru**

[3] Financial University under the Government of the Russian Federation, 49/2, Leningradsky ave., Moscow, 125167, Russia, *e-mail:* **7283763@mail.ru**

[4] Lomonosov Moscow State University, 1, Leninskie Gory, Moscow, 119991, Russia, *e-mail:* **vstikunov@yandex.ru**

[5] Lomonosov Moscow State University, 1, Leninskie Gory, Moscow, 119991, Russia, *e-mail:* **irina.tikunova@icloud.com**

Space monitoring in conditions of increased risk of emergencies of a natural and man-made nature and the involvement of medical and preventive measures to maintain the health of the population (flora, fauna) in critical situations is a global, urgent task [*Nadudvari*, 2014; *Manzo*, 2016; *Kazaryan*, *Voronin*, 2021].

When performing monitoring, periodic observation of a fixed section of the study area is necessary. Photographic surveys from an Earth satellite are exposed to external factors that interfere with obtaining objective information — the state of the atmosphere, the season of the year, the position of the sensor, etc. To get out of the situation, additional procedures are used: atmospheric correction, creation of index images, normalization. They are performed during filming and this is inconvenient in terms of additional time and material costs [*Schovengerdt*, 2013].

It is necessary to look for another way to solve the problem, and this solution is to use the apparatus of discrete orthogonal transformations (DOT) [*Hall*, 1967; *Gonzalez*, 2019; *Umnyashkin*, 2021].

It should be noted that the main reasons for the increased interest in the study and application of DOT are related to the transition to a new reference system in the spectral region, linearity, reversibility and energy conservation, which is characteristic of orthogonal transformations, the presence of effective fast algorithms, etc. [*Golubov* et al., 2008].

Aerospace research problems are faced with the problem of reducing redundancy and efficient coding (data compression), which arises in connection with the processing of huge flows of information presented in the form of digital signals.

The task of compressing space images and discarding non-informative elements leads to an increase in brightness, which is the main feature in recognizing municipal solid waste (MSW) using GIS associated with images on the Earth's surface. The problems of constructing and using data compression systems are closely related to the automation of scientific research. In this regard, the task of data compression, being the main means of increasing the efficiency of space image processing, acquires great practical importance.

There are two main methods for selecting spectral components: zonal and threshold. Zonal selection consists of isolating a set of components occupying certain fixed areas of the spectrum, and the threshold compression method preserves only those spectral components whose value exceeds a set threshold. Threshold coding systems provide a more correct choice of transmitted samples (in terms of the magnitude of distortion), but they have disadvantages, in particular, the need to encode additional information about the addresses of transmitted samples. So, we will investigate the following problem.

Task. Find such a DOT for a given class of signals *(N* — dimensional random vectors) such that the signal reconstructed from M ($M < N$) spectrum components has a minimum (in the sense of root-mean-square) deviation from the input.

As is known [*Golubov* et al., 2008], this problem has an analytical solution and this is the Karunen-Loewe transformation (K-L), which is built on the basis of the eigenfunctions of the covariance matrix K. In applied problems, its use is not advisable due to the fact that it is necessary to perform a large number of calculations: $O(N^3)$ operations to determine the eigenfunctions K and $O(N^2)$ operations for the transformation itself.

For applied problems, Fourier transforms, real trigonometric transforms of Hadamard, Walsh, Haar, etc., which have fast algorithms, are widely used (FA).

In this work we will consider Fibonacci DOT (DTFb) [*Stakhov*, 1981, 1984]. Of course, these transformations cannot represent some alternative to the classical DOT, but in some cases they have useful applications [*Fraenkel*, 1985, 1989].

RESEARCH MATERIALS AND METHODS

Preliminary studies: properties of the Fibonacci Transformation

Let's consider orthogonal Fibonacci transformations [*Agaian*, *Alaverdian*, 1988; *Agaian* et al., 1988; *Bertrand-Mathis*, 1989; *Agaian*, 1990; *Bergman*, 1997].

Fibonacci transformation. Let $\varphi_0(x)$ integrated on $[0,1)$ function, N natural number, $\Delta_i = \left[\frac{i-1}{N}, \frac{i}{N}\right)$, $i=1,2,\text{K},N$. Fair ratio $\bigtimes_{i=1}^{N} \Delta_i = [0,1)$.

Let us introduce a number of notations (1):

$$\varphi_1(x) = \begin{cases} \varphi_0(x) & by \quad x \in \Delta_1 \\ -\varphi_0(x) & by \quad x \in \Delta_2 \\ 0 & by \quad x \in \bigtimes_{i=3}^{N} \Delta_i \end{cases} \tag{1}$$

$$\varphi_k(x) = \begin{cases} \varphi_i(x) & by \quad x \in \Delta_i,\ i = \overline{1,k} \\ -\left[\varphi_{k-1}(x) + \varphi_{k-2}(x)\right] & by \quad x \in \Delta_{k+1} \\ 0 & by \quad x \in \bigtimes_{i=k+2}^{N} \Delta_i \end{cases}$$

Function system $\{\varphi_k(x)\}$, $k = \overline{0,N}$ called the Fibonacci system. The Fibonacci system is orthogonal (proof below), but not orthonormal. Let's introduce another system (2) and we will also call it the Fibonacci system:

$$\Phi_{i,k}(x) = \begin{cases} \frac{\varphi_k(x)}{\sqrt{\varphi_i(x)\varphi_{i+2}(x)}} & by \quad x \in \bigcup_{i=1}^{k+1} \Delta_i \\ 0 & by \quad x \in \bigcup_{i=k+2}^{k+1} \Delta_i, \quad i = \overline{1,N-1}, \quad k = \overline{1,N} \end{cases} \tag{2}$$

$\Phi_{N,k}(x) = \frac{\varphi_k(x)}{\sqrt{\varphi_N(x)\varphi_{N+1}(x)}}$ $k = \overline{1,N}$, where $\varphi_{n+1}(x) = \varphi_{n-1}(x) + \varphi_n(x)$, $n = 2,3,\text{K}$

This system with $\varphi_0 = const$ is orthonormal. The proof of this statement is given below.

Let us introduce the concept of a discrete Fibonacci function. For a natural number N, we define the functions $\varphi_N(x,k)$:

$$\varphi_N(x,k) = \varphi_k\left(\frac{2x+1}{2N}\right), \quad x = 0,1,\text{K}, N-1, \quad k = 1,\text{K}, N$$

and matrix (3):

$$\varphi_N = \left\| \varphi_N(x, k) \right\|, \; x = 0,1,\text{K}, \; N-1, \;\; k = 1,\text{K}, \; N \tag{3}.$$

Let's call it the Fibonacci matrix. Here is a general view of the Fibonacci matrix (4):

$$\Phi_N = \begin{bmatrix} \varphi_1 & -\varphi_1 & 0 & 0 & \Lambda & \Lambda & \Lambda & 0 & 0 \\ \varphi_1 & \varphi_2 & -\varphi_2 & 0 & \Lambda & \Lambda & \Lambda & 0 & 0 \\ \varphi_1 & \varphi_2 & \varphi_3 & -\varphi_3 & \Lambda & \Lambda & \Lambda & 0 & 0 \\ \Lambda & \Lambda & \Lambda & \Lambda & \Lambda & \Lambda & \Lambda & \Lambda & \Lambda \\ \varphi_1 & \varphi_2 & \varphi_3 & \Lambda & \varphi_i & -\varphi_i & \Lambda & 0 & 0 \\ \text{K} & \Lambda & \Lambda & \Lambda & \Lambda & \Lambda & \Lambda & \Lambda & \Lambda \\ \varphi_1 & \varphi_2 & \varphi_3 & \Lambda & \Lambda & \Lambda & \Lambda & \varphi_{N-1} & -\varphi_{N-1} \\ \varphi_1 & \varphi_2 & \varphi_3 & \Lambda & \Lambda & \Lambda & \Lambda & \varphi_{N-1} & \varphi_N \end{bmatrix} \tag{4}$$

Let us present the Fibonacci matrix corresponding to the orthonormal Fibonacci system for the case of $N = 8$ as an example.

$$\Phi_8 = \begin{bmatrix} 1/\sqrt{2} & (1 & -1 & 0 & 0 & 0 & 0 & 0 & 0) \\ 1/\sqrt{3} & (1 & 1 & -1 & 0 & 0 & 0 & 0 & 0) \\ 1/\sqrt{10} & (1 & 1 & 2 & -2 & 0 & 0 & 0 & 0) \\ 1/\sqrt{24} & (1 & 1 & 2 & 3 & -3 & 0 & 0 & 0) \\ 1/\sqrt{65} & (1 & 1 & 2 & 3 & 5 & -5 & 0 & 0) \\ 1/\sqrt{168} & (1 & 1 & 2 & 3 & 5 & 8 & -8 & 0) \\ 1/\sqrt{442} & (1 & 1 & 2 & 3 & 5 & 8 & 13 & -13) \\ 1/\sqrt{714} & (1 & 1 & 2 & 3 & 5 & 8 & 13 & 21) \end{bmatrix}$$

Let us list the main properties of the Fibonacci system.

Property № 1. System $\{\varphi_k(x)\}$, $k = \overline{1,N}$ is orthogonal on $[0,1)$. Proof:

If $k < m$, then

$$\int_0^1 \varphi_k(x)\, \varphi_m(x) dx = \sum_{i=1}^{k+1} \int_{\Delta_i} \varphi_k(x)\, \varphi_m(x) dx \tag{5}$$

According to the statement $\varphi_k(x)$ (1), we will have:

$$\varphi_k(x) = \varphi_m(x) \text{ by } \; x \in \bigcup_{i=1}^{k} \Delta_i,$$

$$\varphi_k\ (x) = 0 \text{ by } \ x \in \bigcup_{i=k+2}^{N} \Delta_i\ ,$$

From here it goes,

$$\sum_{i=1}^{k+1} \int_{\Delta_i} \varphi_k\ (x)\, \varphi_m\ (x) = \ \frac{1}{N} \sum_{i=1}^{k} \varphi_i^2\ - \int_{\Delta_{k+1}} \varphi_k\,(x) \varphi_{k+1}\,(x) dx\ = \frac{1}{N} \left[\sum_{i=1}^{k} \varphi_i^2\ - \varphi_k\, \varphi_{k+1} \right] \quad (6),$$

where φ_i — meaning $\varphi_i(x)$ on interval Δ_i.

In interval Δ_i, $\varphi_i\,(x)$, $i = \overline{1,\ N}$ are constantly and define by $\varphi_i = \varphi_{i-1} + \varphi_{i-2}$, in other words are numbers of Fibonacci. Therefore, the equality is true (7):

$$\sum_{i=1}^{k} \varphi_i^2 = \varphi_k\ \ \varphi_{k+1} \qquad (7)$$

With looking on (6) and (7) statement (5) among zero. Therefore, system $\varphi_k\,(x)$, $k = \overline{1,\ N}$ — is orthogonal.

Property № 2. System $\Phi_{i,k}\,(x),\ k = \overline{1, N}$ — is orthonormal (proof similar to point 1).

Property № 3. Let $\alpha = \frac{1+\sqrt{5}}{2}$, $\beta = \frac{1-\sqrt{5}}{2}$, и $\varphi_k\,(x) = \dfrac{\alpha^{\,k} - \beta^{\,k}}{\sqrt{5}}$, $k = 1, 2, \text{K}$ (Binet formula [*Stakhov*, *Luzhnetsky*, 1981]), then the Fibonacci matrix at $\varphi_0 = 1$ looks like:

$$\Phi_N = \frac{1}{\sqrt{5}} \begin{bmatrix} \frac{\alpha-\beta}{\sqrt{(\alpha-\beta)(\alpha^3-\beta^3)}} & -\frac{\alpha^2-\beta^2}{\sqrt{(\alpha-\beta)(\alpha^3-\beta^3)}} & \Lambda & 0 & 0 \\ \frac{\alpha-\beta}{\sqrt{(\alpha^2-\beta^2)(\alpha^4-\beta^4)}} & \frac{\alpha^2-\beta^2}{\sqrt{(\alpha^2-\beta^2)(\alpha^4-\beta^4)}} & \Lambda & 0 & 0 \\ \Lambda & \Lambda & \Lambda & \Lambda & \Lambda \\ \frac{\alpha-\beta}{\sqrt{(\alpha^{n-1}-\beta^{n+1})(\alpha^{n+1}-\beta^{n+1})}} & \Lambda & \Lambda & 0 & \frac{\alpha^n-\beta^n}{\sqrt{(\alpha^n-\beta^n)(\alpha^{n+1}-\beta^{n+1})}} \end{bmatrix}$$

Let $\{\varphi_k\}$ — sequence of numbers, then α, β — positive real numbers, and for any n the following relation holds:

$$\varphi_n\, \varphi_{n+1}\ = \alpha \sum_{\mathrm{k=1}}^{\mathrm{n}} \beta^{\mathrm{n-k}}\ \varphi_k^2\ ,$$

then the Fibonacci matrix looks like (8):

$$\Phi_N(\alpha,\beta)=\begin{bmatrix} \frac{\alpha\,\varphi_1}{\sqrt{\varphi_1\varphi_3}} & -\frac{\sqrt{\beta}\,\varphi_1}{\sqrt{\varphi_1\varphi_3}} & 0 & 0 & \Lambda & 0 & 0 \\ \frac{\alpha\sqrt{\beta}\,\varphi_1}{\sqrt{\varphi_2\varphi_4}} & \frac{\alpha\ \varphi_2}{\sqrt{\varphi_2\varphi_4}} & -\frac{\beta\ \varphi_2}{\sqrt{\varphi_2\varphi_4}} & 0 & \Lambda & 0 & 0 \\ \Lambda & \Lambda & \Lambda & \Lambda & \Lambda & \Lambda & \Lambda \\ \frac{\alpha\left(\sqrt{\beta}\right)^{n-2}\varphi_1}{\sqrt{\varphi_{n-1}\varphi_{n+1}}} & \frac{\alpha\left(\sqrt{\beta}\right)^{n-2}\varphi_2}{\sqrt{\varphi_{n-1}\varphi_{n+1}}} & \Lambda & \Lambda & \frac{\alpha\,\varphi_{n-1}}{\sqrt{\varphi_{n-1}\varphi_{n+1}}} & -\frac{\alpha\sqrt{\beta}\,\varphi_{n-1}}{\sqrt{\varphi_{n-1}\varphi_{n+1}}} & 0 \\ \frac{\sqrt{\alpha}\left(\sqrt{\beta}\right)^{n-1}\varphi_1}{\sqrt{\varphi_n\varphi_{n+1}}} & \frac{\sqrt{\alpha}\left(\sqrt{\beta}\right)^{n-2}\varphi_2}{\sqrt{\varphi_n\varphi_{n+1}}} & \Lambda & \Lambda & \frac{\sqrt{\alpha}\sqrt{\beta}\,\varphi_{n-1}}{\sqrt{\varphi_n\varphi_{n+1}}} & \frac{\sqrt{\alpha}\,\varphi_n}{\sqrt{\varphi_n\varphi_{n+1}}} & -5 \end{bmatrix} \tag{8}$$

Property № 4. $\Phi_N\,\Phi_N^T = I_N$.

Property № 5. The determinant of a Fibonacci matrix of order *N* is equal to the product of the diagonal elements and the number φ_{n+1}, those first *N + 1* Fibonacci numbers.

$$\det\|\varphi_n\| = \prod_{i=1}^{N+1}\varphi_i \quad ,\ \det\|\Phi_N\| = 1 \tag{9}$$

Property № 6. For the practical application of DOT, it is important to have a way to quickly calculate it, a fast conversion algorithm. The main criterion for an algorithm when implemented on a computer is the number of arithmetic operations. Direct (10) and inverse (11) Fibonacci transformations have the form:

$$Y = \Phi_N\,X \tag{10},$$

$$x = \Phi_N^{-1}\,Y = \Phi_N^T\,Y \tag{11},$$

where $X = (x_1, x_2, \text{K}, x_n)$ — input vector (signal),

Φ_N — the Fibonacci matrix corresponding to the orthonormal Fibonacci system.

Let's look at these algorithms in detail. From (7) we have:

$$y_i = \sum_{k=1}^{i}\Phi_k\,x_k - \Phi_i\,x_{i+1}\ , \qquad \Phi_k = \frac{\varphi_k}{\sqrt{\varphi_k\ \varphi_{k+2}}}\ ,\ k = \overline{1,\ N-2}\ .$$

From here we will have the following recurrent formula:

$$y_{i+1} = \sum_{k=1}^{i+1}\Phi_k\,x_k - \Phi_{i+1}\,x_{i+2} = \sum_{k=1}^{i}\Phi_k\,x_k - \Phi_i\,x_{i+1} + \Phi_{i+1}\,x_{i+1} - \Phi_{i+1}\,x_{i+2} + \Phi_i\,x_{i+1} =$$
$$= y_i + x_{i+1}(\Phi_i + \Phi_{i+1}) - \Phi_{i+1}\,x_{i+2} = y_i + \Phi_{i+2}\,x_{i+1} - \Phi_{i+1}\,x_{i+2}\ ,$$
$$y_1 = \Phi_1(x_1 - x_2)$$

So,

$$y_{i+1} = y_i + \Phi_{i+2}\, x_{i+1} - \Phi_{i+1}\, x_{i+2}\ , \qquad i = \overline{1,\ N-2} \tag{12}$$

$$y_1 = \Phi_1 \left(x_1 - x_2\right)$$

$$y_N = y_i + \Phi_{N+1}\, x_N\ , \qquad \Phi_{N+1} = \frac{\varphi_{N+1}}{\sqrt{\varphi_N\ \varphi_{N+1}}}\ .$$

Fig. 1a shows the algorithm of the direct fast Fibonacci transformation for $N = 8$. Let's consider the Fibonacci inverse transformation algorithm. From (11) we have:

$$x_i = -\frac{\varphi_{i-1}}{\sqrt{\varphi_{i-1}\ \varphi_{i+1}}}\ y_{i-1} + \varphi_i \left(\sum_{k=i}^{N-1} \frac{y_k}{\sqrt{\varphi_k\, \varphi_{k+2}}} + \frac{y_k}{\sqrt{\varphi_N\, \varphi_{N+1}}} \right)\ , \quad i = \overline{N-2,\ 2} \tag{13}$$

Let

$$T_i = \sum_{k=0}^{N-1} \frac{y_k}{\sqrt{\varphi_k\ \varphi_{k+2}}} + \frac{y_N}{\sqrt{\varphi_N\ \varphi_{N+1}}}\ , \qquad i = \overline{N-1,\ 2} \tag{14}$$

Expression (14) is represented as follows:

$$T_{i-1} = T_i + \frac{y_{i-1}}{\sqrt{\varphi_{i-1}\ \varphi_i}}\ .$$

So,

$$x_{i-1} = \frac{\varphi_{i-2}}{\sqrt{\varphi_{i-2}\ \varphi_i}}\ y_{i-2} + \varphi_{i-1}\ T_{i-1}\ , \qquad i = \overline{N,3}$$

$$x_1 = T_1 + \frac{y_1}{\sqrt{2}}$$

$$x_N = -\frac{\varphi_{N-1}}{\sqrt{\varphi_{N-1}\ \varphi_{N+1}}} + \frac{y_N\ \varphi_N}{\sqrt{\varphi_N\ \varphi_{N+1}}} \tag{15}$$

Formula (14) is a fast inverse transformation scheme for $N = 8$, where:

$$g_i = \frac{\varphi_i}{\sqrt{\varphi_{i-1}\ \varphi_{i+1}}}\ , \quad i = \overline{1,\ N-1}\ , \quad g_N = \frac{\varphi_n}{\sqrt{\varphi_n\ \varphi_{n+1}}}\ r_i = \frac{g_i}{\varphi_i}\ , \quad i = \overline{1,\ N}$$

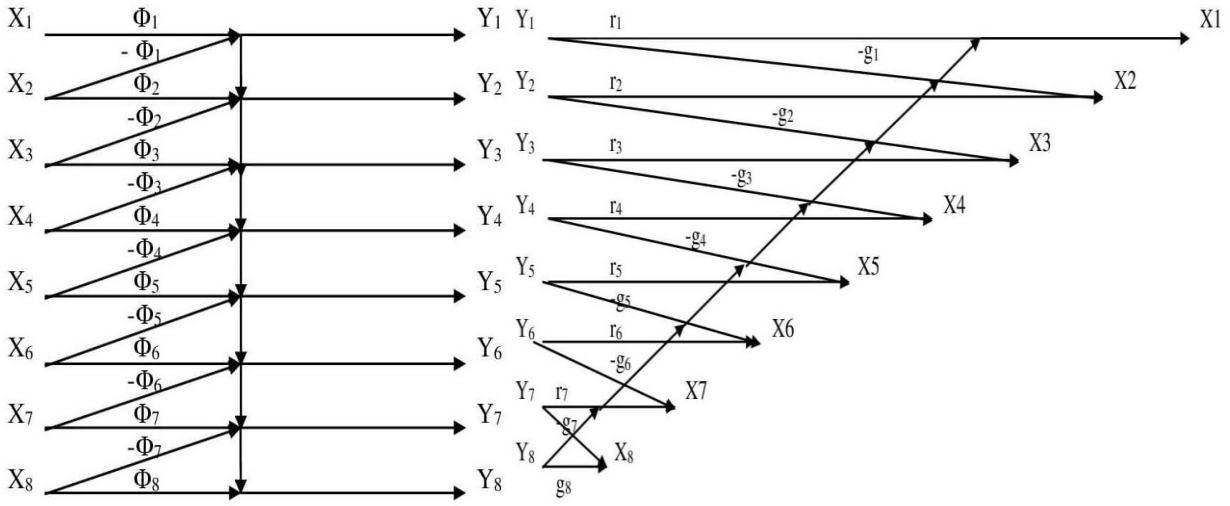

a) Fast direct Fibonacci conversion algorithm

b) Fast Fibonacci inverse transformation algorithm

Fig. 1. Representation of the fast Fibonacci transformation algorithm for N = 8

Property № 7. The complexity of calculating the forward and reverse Fibonacci transformations. The lower bound of the complexity of algorithms [*Golubov* et al., 2008] calculating the orthogonal transformation based on the basis of *F* is estimated:

$$\mu^{+}L^{+} + \mu^{\times}L^{\times} \geq \frac{\log\left(\left|\Delta F\right|\right)}{\log\left(2A\right)} \qquad (16),$$

where μ^{+} and $\mu^{\times}$ — weighty coefficients,

L^{+} and $L^{\times}$ — the number of additions and subtractions.

$$\Delta F = \max_{i,j}\left\{\Delta F_{i,j}\right\},$$

where $\Delta F_{i,j}$ — the determinant of the minor of the matrix *F*.

$$A \geq \max_{j}\left\{\left|\lambda_j\right|, \left|\mu_j\right|\right\},$$

where λ_j and μ_j — constants used in the class of algorithms that calculate the transformation *F*.

For the discrete Fibonacci transformation:

$$\Delta F = \prod_{i=1}^{N+1}\varphi_i \quad , \quad A = \varphi_N .$$

For convenience, instead of $\left\{\varphi_n\right\}\ n = \overline{1,N}$ we will consider the basic functions $\left\{\sqrt{5}\ \varphi_n\right\}\ n = \overline{1,N}$.

Fibonacci numbers $\{\varphi_n\}\ n=\overline{1,N}$ is the nearest integer to the number $\frac{\alpha^n}{\sqrt{5}}$, where $\alpha=\frac{1+\sqrt{5}}{2}$; then you can write:

$$\log\left(\Delta F\right)=\sum_{n=1}^{N+1}\log\left(\sqrt{5}\ \varphi_n\right)=\left[\log\alpha\sum_{n=1}^{N+1}n\right]=\left[\ \log\alpha\cdot\frac{\left(N+1\right)\left(N+2\right)}{2}\right],$$

and so on:

$$\mu^{+}L^{+}\ +\ \mu^{\times}L^{\times}\ \geq\left[\frac{\left(N+1\right)\left(N+2\right)}{2\left(1+N\log\alpha\right)}\cdot\log\alpha\right] \tag{17}$$

Let $C=L^{+}+L^{\times}$. It follows from (12) and (15) that with a direct transformation $L^{+}=2N-2$, $L^{\times}=2N-1$, and with the reverse conversion $L^{+}=2N-2$, $L^{\times}=2N$. Therefore,

$$\frac{N}{2}+1\leq C\leq 4N-3$$

Property № 8. The Karunen-Loew transform and the Fibonacci transform. When solving our task of decrypting satellite images in order to monitor for the presence of household waste, we will use the Fibonacci transform (instead of the Karunen-Loew transform). The basis for such a decision is the following statement [*Agaian*, 1990; *Agaian*, *Alaverdian*, 1996].

Statement. Let f_N — a random signal with a covariance matrix

$$\begin{gathered}K=\left\{k_{m,n}\right\},\ m,n=\overline{1,N}\\ k_{m,n}=\tfrac{1}{N}\sum_{j=1}^{N}r_{m,j}\,r_{n,j}\quad,m,n=\overline{1,N}\end{gathered} \tag{18},$$

where

$$r_{ij}=\sqrt{N}\sum_{t=1}^{N}\frac{\varphi_t\sqrt{\lambda_t}}{\sqrt{\varphi_i\,\varphi_{i+2}}}\,h_{t\,j}\ \ i,j=\overline{1,N} \tag{19},$$

$$h_{\,t,j}=\left(-1\right)^{\sum_{l=0}^{P-1}k_l\,j_l}\ ,\ \lambda_t\ \geq 0,\ t=\overline{1\ N} \tag{20},$$

$\left(t_0,\ t_1,\text{K}\ ,\ t_{p-1}\right)$ and $\left(j_0,\ j_1,\text{K}\ ,\ j_{p-1}\right)$ — binary representations of numbers $t-1$ and $j-1$.

Then it's fair (21):

$$K_N \Phi_N = \Phi_N \Lambda_N, \ \Lambda_N = diag(\lambda_1, \lambda_2, \text{K}, \lambda_n) \quad (21)$$

Proof. The expression (17) is presented in the following form:

$$r_{ij} = \sqrt{N} \sum_{t=1}^{N} \frac{\varphi_{i,t}}{\sqrt{\varphi_{i,t} \ \varphi_{i+2,t}}} \sqrt{\lambda_{t,j}} \ h_{t,j} \ \ i, j = \overline{1, N},$$

where

$$\varphi_{i,t} = \varphi_t \quad , \quad \lambda_{t,j} = \lambda_t$$

In matrix form, you can write this expression as (22):

$$R_N = \sqrt{N} \Phi_N \Lambda_N^{1/2} H_N \quad (22),$$

where H_N — the Walsh-Hadamard matrix of order *N*.

Given (20), we write (16) as (23):

$$K_N = \frac{1}{N} R_N R_N^T \quad (23)$$

Substitute (21) in the left part of equation (19):

$$\frac{1}{N}\left(\sqrt{N} \ \Phi_N \Lambda_N^{1/2} \ H_N\right)\left(\sqrt{N} \ H_N^T \Lambda_N^{1/2} \ \Phi_N^T\right)\Phi_N = \Phi_N \Lambda_N^{1/2} \ H_N \ H_N^T \Lambda_N^{1/2} \ \Phi_N^T \Phi_N = \Phi_N \ \Lambda_N,$$

This was exactly what needed to be proved.

Property № 9. It is known that [*Ivashko*, 1983] the *i*-th Fibonacci number can be obtained as a solution to a linear difference equation:

$$\varphi_i - \varphi_{i-1} - \varphi_{i-2} = 0;$$

$$\varphi_i = \frac{\sqrt{5}}{5}\left(\alpha^i - \beta^i\right)$$

$$\alpha = \frac{1+\sqrt{5}}{2} \approx 1{,}618$$

$$\beta = \frac{1-\sqrt{5}}{2} \approx -0{,}618$$

Function $y_1(i) = \alpha^i$ — is an increasing exponent, and $y_2(i) = \beta^i = (-1)^i (0.618)^i$ — alternating decaying sequence.

$$\lim_{i\to\infty}\varphi_i=\frac{\sqrt{5}}{5}\left(\alpha^i-\beta^i\right)=\frac{\sqrt{5}}{5}\alpha^i.$$

In [*Ivashko*, 1983] it is proved that

$$\lim_{\substack{i\to\infty\\N\to\infty}}\sum_{j=1}^{N}\varphi_i(j)=\begin{cases}1, & i<N\\ \alpha^{\frac{3}{2}}\approx 2.058, & i=N\end{cases} \tag{24}$$

The lag, shift, and convolution theorems do not hold for the Fibonacci basis, but Parseval's equality holds.

Here is a mathematical formulation of the problem of information compression by means of the Fibonacci addition. Let's consider the implementation of some random process with certain quantitative characteristics (mathematical expectation = 0, and covariance matrix $\sum_{\bar{x}}$) and we denote this vector of dimension N as follows — $\bar{x}=\left(x_0,\text{K},x_{N-1}\right)$.

We have a non-degenerate matrix of basic functions of some orthogonal system $\left\{\varphi_k(t)\right\}_{k\geq 0}$, on the basis of which an orthogonal transformation is formed F (25):

$$F=\begin{bmatrix}\varphi_0(0) & \varphi_0(1) & \text{K} & \varphi_0(N-1)\\ \varphi_1(0) & \varphi_1(1) & \text{K} & \varphi_1(N-1)\\ \text{K} & \text{K} & \text{K} & \text{K}\\ \varphi_{N-1}(0) & \varphi_{N-1}(1) & \text{K} & \varphi_{N-1}(N-1)\end{bmatrix} \tag{25}$$

Let

F^{-1} is a reverse conversion;

S is the matrix of choice of rank m, where $1\leq m\leq N$ dimensions $m\times N$;

W is the dimension recovery matrix $N\times m$.

The task is to choose F_0, S_0, W_0, satisfying the following conditions:

$$\rho\left(\bar{x},F^{-1}WSF\bar{x}\right)\to\min.$$

Here, ρ is the specified metric.

Let's present the algorithm of the problem in the form of the following flowchart (Fig. 2).

The task is to find the optimal method of zone coding. If $k=N/N_0$ is given, then such spectral components are replaced by zeros, in which the recovery error is minimized:

$$\varepsilon^*=\sup_{\bar{x}\in(X,\rho)}\varepsilon.$$

Consider the following set of vectors with real components (26):

$$X_\Delta=\left\{\bar{x}=\left(x_0,x_1,\text{K},x_{N-1}\right):\ \max_k\left|x_{k-1}-x_k\right|\leq\Delta\right\} \tag{26},$$

where $N = r^n$,

and the vector $\bar{y}_s = \left(0,\text{K} , 0, y_{r^s} , y_{r^s+1} ,\text{K} , y_{r^{s+1}} ,0,\text{K} ,0 \right)$ $s=0,\text{K} ,n-1$ — is s-th pack of vector y.

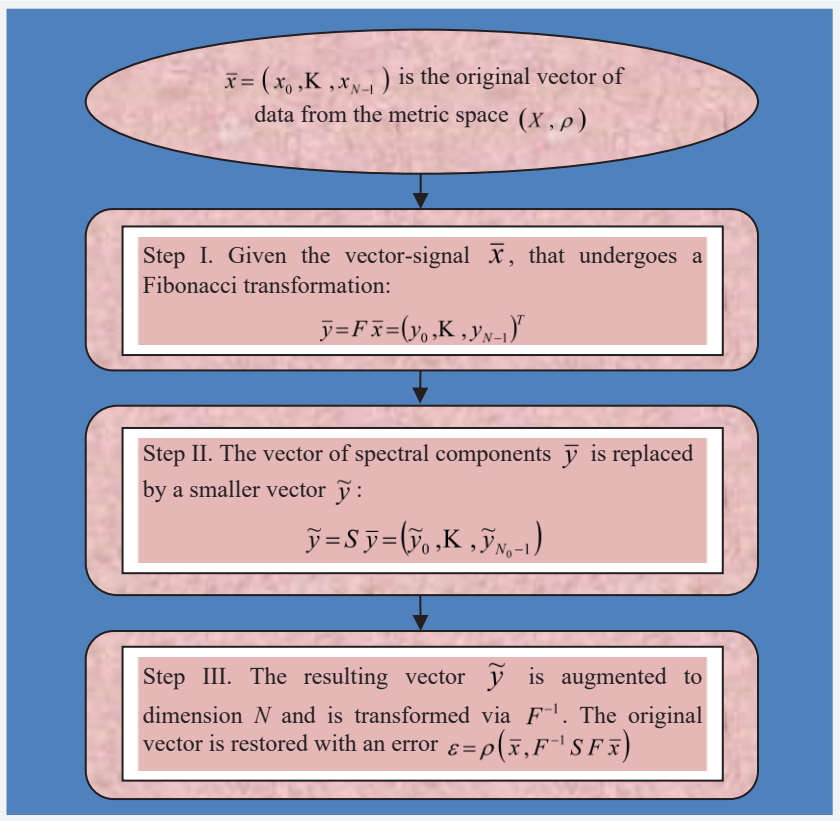

Fig. 2. The algorithm of the problem of finding the optimal method of zone coding in data compression by means of the Fibonacci transformation

To determine the optimal method of zone encoding during compression using the Fibonacci transform, it is necessary to investigate the following extreme problem: $y_j \to extr$ on condition $\bar{x} \in X_\Delta$, where

$$y_j = x_0 \varphi_j (0) + x_1 \varphi_j (1) + x_{N-1} \varphi_j (N-1) \quad (1 \le j \le N-1)$$

To solve this problem, it is necessary to use the principle of optimality in dynamic programming [*Lezhnev*, 2017]. The dynamic planning process will be carried out in the opposite direction, i. e. a decision will be made from the end to the beginning.

Let (27) be the maximum task:

$$y_j \to \max \text{ on condition } \bar{x} \in X_\Delta, \text{ т. е. } |x_{k-1} - x_k| \le \Delta, \quad k = \overline{1, N-1} ,$$

where

$$y_j = x_0 \varphi_j(0) + x_1 \varphi_j(1) + x_{N-1} \varphi_j(N-1) \quad (1 \le j \le N-1) \tag{27}$$

Let $\hat{x}_0$, K , $\hat{x}_{N-2}$ in task (28) be selected. Then the last step is to choose x_{N-1} provided that $| x_{N-2} - x_{N-1} | \le \Delta$. Let us say:

$$\hat{x}_{N-1} = \hat{x}_{N-2} + \Delta \cdot sign\, \varphi_j(N-1) \tag{28}$$

The solution of problem (28) after substitution (29) will have the form:

$$\hat{y}_j = \hat{x}_0 \varphi_j(0) + \hat{x}_1 \varphi_j(1) + \text{K} + \hat{x}_{N-2} \varphi_j(N-2) + \left[\hat{x}_{N-2} + \Delta \cdot sign\, \varphi_j(N-1) \right] \varphi_j(N-1) =$$
$$= \hat{x}_0 \varphi_j(0) + \hat{x}_1 \varphi_j(1) + \text{K} + \hat{x}_{N-2} \left[\varphi_j(N-2) + \varphi_j(N-1) \right] + \Delta \cdot | \varphi_j(N-1) |$$

Now consider the following task (29):

$$y_j \to \max \text{ with task } \bar{x} \in X_\Delta, \text{ so } | x_{k-1} - x_k | \le \Delta, \quad k = \overline{1, N-2} \tag{29},$$

where

$$y_j = \sum_{i=0}^{N-3} x_i \varphi_j(i) + x_{N-2} \left[\varphi_j(N-2) + \varphi_j(N-1) \right] + \Delta \cdot | \varphi_j(N-1) | \quad (1 \le j \le N-2).$$

Let's assume that $\hat{x}_0$, K , $\hat{x}_{N-3}$ in the problem (30) are optimal, then:

$$\hat{x}_{N-2} = \hat{x}_{N-3} + \Delta \cdot sign \left[\varphi_j(N-2) + \varphi_j(N-1) \right],$$

and the solution of the problem (30) will look like:

$$\hat{y}_j = \hat{x}_0 \varphi_j(0) + \hat{x}_1 \varphi_j(1) + \text{K} + \hat{x}_{N-3} \varphi_j(N-3) + \left[\hat{x}_{N-3} + \Delta \cdot sign \left(\varphi_j(N-2) + \varphi_j(N-1) \right) \right] \times$$
$$\times \left[\left(\varphi_j(N-2) + \varphi_j(N-1) \right) \right] + \Delta | \varphi_j(N-1) | = \hat{x}_0 \varphi_j(0) + \hat{x}_1 \varphi_j(1) + \text{K} + \hat{x}_{N-3} \left[\varphi_j(N-3) \right] +$$
$$+ \varphi_j(N-2) + \varphi_j(N-1) + \Delta | \varphi_j(N-2) + \varphi_j(N-1) | + \Delta | \varphi_j(N-1) |$$

Continuing this process, we have that with the optimal choice of components $\hat{x}_1, \hat{x}_2, \text{K} , \hat{x}_{N-1}$, satisfying the conditions of the problem (30), we will have:

$$\max_{\bar{x} \in X_\Delta} y_j = x_0 \cdot \sum_{i=0}^{N-1} \varphi_j(i) + \Delta \cdot \sum_{m=1}^{N-1} \left| \sum_{i=m}^{N-1} \varphi_j(i) \right| , \quad j = \overline{1,\ N-1} \tag{30}$$

According to the orthogonality of the matrix DTFb and the presence of rows consisting of identical non-zero elements, we have:

$$\sum_{i=0}^{N-1} \varphi_j(i) = 0 \ , \qquad j = \overline{1,\ N-1} \tag{31}$$

Taking into account (32), we will have:

$$\max_{\bar{x} \in X_\Delta} y_j = \Delta \cdot \sum_{m=1}^{N-1} \left| \sum_{i=0}^{m-1} \varphi_j(i) \right| \ , \quad j = \overline{1,\ N-1} \tag{32}$$

Considering task (30) as a minimum task, we get (33):

$$\min_{\bar{x} \in X_\Delta} y_j = -\Delta \cdot \sum_{m=1}^{N-1} \left| \sum_{i=0}^{m-1} \varphi_j(i) \right| \ , \quad j = \overline{1,\ N-1} \tag{33}$$

From (33) and (34) it follows for the Fibonacci matrix $F = \| \varphi_j(i) \|_{j,i=\overline{0,\ N-1}}$, and the DTFb, so

$$\bar{y} = F x = (y_0, y_1, \text{K}\ , y_{N-1})^T,$$

is right:

$$\max_{\bar{x} \in X_\Delta} |y_j| = \Delta \cdot \sum_{m=1}^{N-1} \left| \sum_{i=0}^{m-1} \varphi_j(i) \right| \ , \quad j = \overline{1,\ N-1} \tag{34}$$

Using the ratio (35), we find the form of the matrix *S* for DTFb.

Statement. Let the original data vector belong to the class of vectors with real components (26) and let *F* be a Fibonacci matrix of order *N* (25). Then, the following inequality holds (35):

$$\max_{\bar{x} \in X_\Delta} |y_j| \le \Delta 2.058\ (N-1) \quad (1 \le j \le N-1) \tag{35}$$

Proof. According to (24), we have:

$$\lim_{\substack{i \to \infty \\ N \to \infty}} \sum_{i=0}^{m-1} \varphi_i(j) = \begin{cases} 1, & i < m-1 \\ \alpha^{\frac{3}{2}} \approx 2.058, & i = m-1 \end{cases} \tag{36}$$

$$\begin{aligned} &\text{With } i < m-1,\ \max_{\bar{x} \in X_\Delta} |y_j| = \Delta(N-1) \\ &\text{With } i = m-1,\ \max_{\bar{x} \in X_\Delta} |y_j| = \Delta 2.058\ (N-1) \end{aligned} \tag{37},$$

This was exactly what needed to be proved.

Corollary 1. When increasing the value of *j*, the value of the spectrum $\bar{y}$ (37) it will increase, i. e. it is a monotonously increasing function, therefore, when compressing, it is necessary to replace the initial components of the vector with zeros $\bar{y}$.

Corollary 2. By virtue of Parseval's equality $\| \bar{x} \|_{l_2} = \| \bar{y} \|_{l_2}$ the ratio (37) makes it possible to determine the maximum value of the DOT error using this additional.

Experiments

Soil degradation is a set of processes that lead to changes in soil functions, quantitative and qualitative changes in their properties, gradual deterioration and loss of fertility. The main cause of soil degradation is an anthropological factor: industrialization, urbanization, pollution with solid and liquid waste, poisoning of the soil with pesticides [*Kazaryan* et al., 2018 (a, b), 2019 (a, b)].

As an experimental part of the article, we investigate the problem of applying discrete orthogonal transformations using the example of the Fibonacci transformation for satellite images obtained from the artificial Earth satellite (ASE) Landsat, for aerospace monitoring of solid waste objects, so multispectral images are used, for example, obtained from Landsat-4–5 TM satellites for a given observation period (OP), usually at least 10 years. Data on the amount of precipitation in the study area for the same period. The images must be geo-linked, atmospherically adjusted and cloud-free. Used channels are 1–7 [*Kazaryan* et al., 2018 (a, b), 2019 (a, b)].

Let's consider as one of the methods of processing multispectral images that allow us to improve the results of decryption, the method of applying orthogonal transformations, in particular, the Fibonacci transformation is considered.

It is known that the bands of multispectral images very often turn out to be correlated [*Shovengerdt*, 2013]. The reason for this correlation may be:

- correlation of spectral properties of objects (this is possible, for example, with low reflectivity of vegetation in the visible part of the spectrum);
- topography (the level of shading due to topographic features can be considered the same in all ranges of registration of reflected solar radiation);
- overlapping of registration ranges (ideally, this factor is excluded when developing a sensor, but in practice this is not always done).

Such a correlation leads to the appearance of redundant information. The goal that we face is to try to get rid of it with minimal errors. First, let's consider the representation of a satellite image using orthogonal transformations. Next, we will consider data compression or the selection of certain features, i. e. we will make the transition to a new basis for measurements in fixed spectral channels.

It is known [*Glumov*, 1967; *Chernov*, 2013; *Chernov*, 2020] that an orthogonal transformation, which, on the one hand, provides a representation of the signal, and on the other hand, is optimal in the sense of the RMS criterion. This is the Karunen-Loew transformation. Let's consider how much more profitable it is to use other additional methods when decrypting satellite images.

The transformation matrix of the orthogonal transformation under study is fixed for a given type of sensor and shooting system, therefore, for each new shooting system, it is necessary to calculate new additional coefficients using the principal component method.

Let's consider the essence of the proposed method. The physical justification for it is as follows. In multispectral shooting systems, the image is formed in accordance with the reflection of electromagnetic energy from objects in narrow spectral zones.

The image in certain channels captures the reflection of the spectral brightness of the source object in a given range of the electromagnetic spectrum, i.e., the energy reflected from the surface

is measured by the camera system and recorded as the brightness of the corresponding image element.

The multispectral image is represented as a matrix (38):

$$P_M = \begin{pmatrix} \overline{P_{11}} & \cdots & \overline{P_{1M}} \\ \vdots & \ddots & \vdots \\ \overline{P_{N1}} & \cdots & \overline{P_{NM}} \end{pmatrix} \quad (38)$$

and contain the k images $P_{(k)}$, each of which represents the brightness values measured in narrow spectral zones (k is the number of channels of the shooting system). Vector $\overline{P_{ij}} = (p_{ij}^1, p_{ij}^2, \cdots, p_{ij}^k)$ contains the brightness values of the elements p_{ij} in each channel of the filming system [*Kazaryan* et al., 2018 (a, b), 2019 (a, b)].

For different objects, the spectral luminances in different ranges of the electromagnetic spectrum, although different, are strongly correlated. Measurements in narrow spectral zones (channels) performed by a multispectral survey system do not eliminate correlation dependence. Thus, the measurement system does not form an orthogonal basis. Orthogonal transformations carry out the transition from the measurement space of spectral brightness of objects to the space of features associated with the properties of a given class of objects.

So, the experiment consists of performing two steps: the first is to apply an orthogonal transformation to the original image, which will make it possible to decorrelate the component vectors of the image and reduce the dimension of the image; the second is to build a trainable classifier to perform the task of pattern recognition.

Let's consider the implementation of the first part, namely, the selection of features.

The type of object that is subject to changes in the presence of solid household waste is considered: clean soil, i. e. we are interested in the sign of brightness.

The purpose of experimental studies is to evaluate the accuracy of soil decryption based on comparing the results of visual decryption from the original image and the image obtained using the DOT, as well as on the basis of comparing the results of classification without training using the K-MEANS algorithm from the original image, from an image with an orthogonal transformation.

After segmenting the selected SI, we define homogeneous clusters.

The further numerical algorithm is defined as follows. Let the initial matrix X of brightness of dimension $N * N$ is the realization of some random process with certain properties. Let's entertain the following notation:

- F — is a discrete orthogonal Fibonacci transformation;
- δ — is the value of the deviation of the original signal;
- F^{-1} — reverse conversion;
- k — is the compression ratio;
- S — is a matrix of choice of dimension $m * N$ of rank m, $1 <= m <= N$

Description of the Algorithm

Let's convert the digital image "X" to the spectral region "Y" as follows: $Y = FX$, where F is a discrete orthogonal Fibonacci transformation. Even if we consider the input signal to be set exactly, then the vector $\overline{Y} = SFX$ to be further processed is distorted. As a result of these actions, the original vector is restored with errors:

$$\varepsilon_1 = \rho_{l2}\,(X, F^{-1}S^T SFX_\delta) \quad (39),$$

where l_2 — is the standard metric.

Using the example of individual transformations, we will evaluate the possibility of using an additional one in the task of recognizing open-type debris areas from satellite images *X*. To do this, for this type of transformation, we will find the matrices $W = F^{-1}SF$, at which the minimum deviation value is reached for a given class of objects (littering areas) $\varepsilon = \rho(WX, C)$, where F^{-1} — is the inverse matrix DOT (in particular, it can be an inverse or pseudo-inverse matrix), $X = f^{-1}(Y) = F^{-1}Y$, S — the matrix of class selection, C — the matrix of selection of reference areas occupied by known MSW in the field of observation, ρ — some norm.

RESEARCH RESULTS AND DISCUSSION

The regression analysis method

Let's find the matrix *W* for the halftone image *X* using the standard deviation method:

$$\varepsilon = \frac{1}{2}\sum_{i,j} a_{ij}^2 \to \min, \quad A = [a_{ij}]_{n*m} = WX - C \tag{40},$$

W is not tied to any type of OT and sets some affine transformation of the original matrix X into the desired matrix C — a binary image of the selection of the test area (element values: 1 — area, 0 — background). For a given image *X* of size $n \times m$, the *W* operator is unique and restores the area *C* with a given accuracy *D*.

Criterion (40) is transformed into a system of equations:

$$\frac{\partial \varepsilon}{\partial a_{ij}} = 0 = \sum_{k=1}^{m} a_{ik} x_{jk} \tag{41}$$

$$a_{ij} = w_{i1}x_{1j} + w_{i2}x_{2j} + \ldots + w_{in}x_{nj} - c_{ij}, \quad i = 1\ldots n, j = 1\ldots m$$

$$X = [x_{ij}]_{n*m}, \quad W = [w_{ij}]_{n*n}, \quad C = [c_{ij}]_{n*m}$$

As a result of solving a system of linear algebraic equations (41) from *mn* equations, we find:

$$W = \left(\left(D \cdot (XC^T)\big|_{n^2*1} \right)_{n*n} \right)^T, \quad D = I_n \otimes B, B = (XX^T)^{-1} \tag{42},$$

where $\otimes$ and $\cdot$ — operations of Kronecker and ordinary matrix products,

$A\big|_{n*m}$ — the operation of transforming the size of the matrix A to size n = m (when moving through the elements in the column directions, starting from the first element),

I_n — a unit matrix of size n.

Matrix of class area allocation according to its standard: $E = WX$.

Discussion of the results of the regression analysis method

Let's look at the example of specific images of the result of the experiment.

Fig. 3 shows an example of the transformation and restoration of the reference area (MSW Kuchino polygon, August 2011). From the figure it can be seen that for the "native" image X, the matrix E = C, and for another X', close in date to the shooting from $X - E' \approx C$.

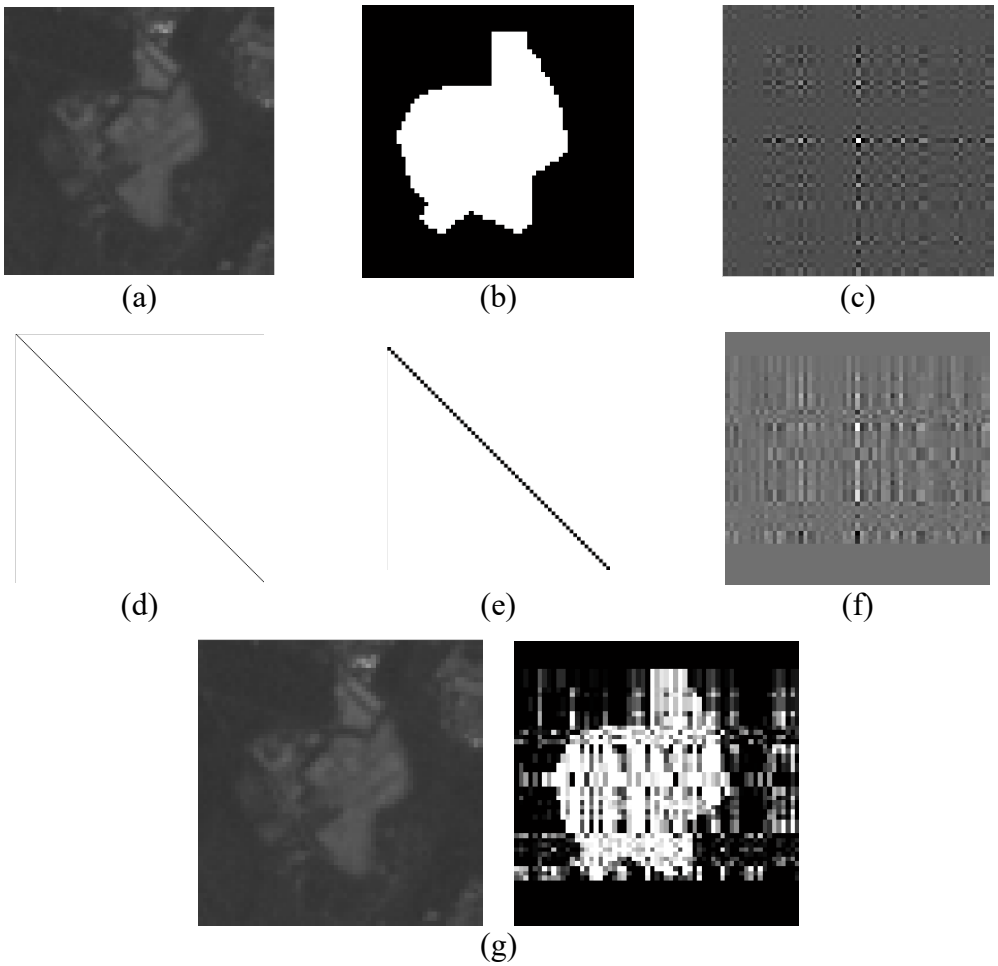

Fig. 3. a) the original image X (n = m = 64); b) the reference C (identical to the matrix E); c) matrix B; d) the unit matrix In; e) the Kronecker product D (diagonal blocks — matrix B); f) matrix W; g) matrix E' for another image X' ($E' \approx E$)

It is clear that the more input images $\{X^k\}$ are taken over a wider observation period T and the more channels $\{X^{lk}\}$, the more accurate the selection of the object on which the standard is built. Then, plus, the more reference areas $\{C^p\}$, the more accurate the selection is not only of all objects on which the corresponding ones are built standards, but also within the limits of the very class of these objects.

More generally, the input matrices X and C: can be obtained through the Kronecker product:

$$X = J_{1*p} \otimes X', C = J_{lk*1} \otimes C', \quad X' = \begin{bmatrix} X^1 \\ \dots \\ X^k \end{bmatrix}, X^k = \begin{bmatrix} X^{1k} \\ \dots \\ X^{lk} \end{bmatrix}, C' = \begin{bmatrix} C^1 & \dots & C^p \end{bmatrix},$$

where $J_{n \times m}$ — matrix of units of size $n \times m$, k — the number of images covering the observation area U during the observation period T, l is the number of channels, p is the number of standards lying on the area U. X^{lk} and C^p — matrices of size $nm \times 1$ (transformation from matrices of size n × m).

Coefficient matrix (the operation of constructing a block diagonal matrix W from the main diagonal w):

$$W = I_n \otimes w = \begin{bmatrix} W^1 & & & \\ & W^2 & & \\ & & \dots & \\ & & & W^k \end{bmatrix}, \quad w = \begin{bmatrix} W^1 & W^2 & \dots & W^k \end{bmatrix},$$

where W — the desired matrix of $nmlk \times nmlk$ size coefficients describing this class of objects; W^k are matrices of $nml \times mnl$ size coefficients obtained for the k-th snapshot.

Block-diagonal matrix $E = I_n \otimes e = WX$, where $e = [E^1\ E^2\ \dots\ E^k]$ will have a size of $mnlk \times 1$. If the OT is not carried out on all channels, but on each separately:

$$W^k = I_l \otimes w^k, E^k = I_l \otimes e^k, W^{lk} = I_m \otimes w^{lk}, w^k = \begin{bmatrix} W^{1k} & W^{2k} & \dots & W^{lk} \end{bmatrix},$$
$$e^k = \begin{bmatrix} E^{1k} & E^{2k} & \dots & E^{lk} \end{bmatrix}, w^{lk} = \begin{bmatrix} W'^{lk} & W'^{lk} & \dots & W'^{lk} \end{bmatrix}.$$

W'^{lk} — coefficient matrices of size $n \times n$ obtained on the l-th channel of the k-th image using the model (42) for $X = J_{1*p} \otimes X^{lk}\big|_{n*m}$ and $C = C'$ (for the "final" OT).

Each W^k matrix identifies a class on a specific day of shooting (chronological, seasonal), detection image: $E^k = W^k X^k$.

The Karunen-Loew transformation

The Karunen-Loew transformation (principal component method) consists in the transition from a system of k old variables (factors) to a system of $k' < k$ new variables (principal components). The original image X, consisting of channels $\{X^l\}$, $l = 1 \dots k$, converted to an image Y, converted to an image $\{Y^l\}$, $l = 1 \dots k'$.

To do this, an OT:

$$Y' = vX', \quad v = \begin{bmatrix} v_1 & v_2 & \dots & v_k \end{bmatrix}^T, \quad X' = \begin{bmatrix} X'^1 & X'^2 & \dots & X'^k \end{bmatrix}^T,$$

where v_l — the eigenvectors of the matrix $C = [c_{ij}]$ of size $k \times k$ (the dimensions of the vectors are $k \times 1$), arranged in descending order of eigenvalues d_l;
c_{ij} — the correlation coefficient between the above factors X'^i and X'^j.

$$X'^i = \frac{X''^i - m_i}{s_i},$$

where m_i and s_i — mathematical expectation and standard deviation of the sample X''^i;
X''^i — vector columns of dimensions $nm \times 1$ obtained by transformation from matrices X^i of dimensions $n \times m$.

From the matrix $Y' = [Y'^1\ Y'^2\ \dots\ Y'^k]$ the first k' < k columns are selected — a matrix of the main components is obtained $Y = [Y'^1\ Y'^2\ \dots\ Y'^{k'}]$. Usually, $k' = 1 \dots 4$.

Discussion of the results of the Karunen-Loew transformation

Fig. 4 shows an example of constructing the main components for a multispectral image of the observation area (Balashikha district, Zheleznodorozhny island, August 2011). Despite the fact that the most significant components are 1–3, the best selection of areas of debris and open soil highlighted in dark blue (d) is given by combination 1 (on the red channel), 2 (on the green channel) and 6 (on the blue channel) main components.

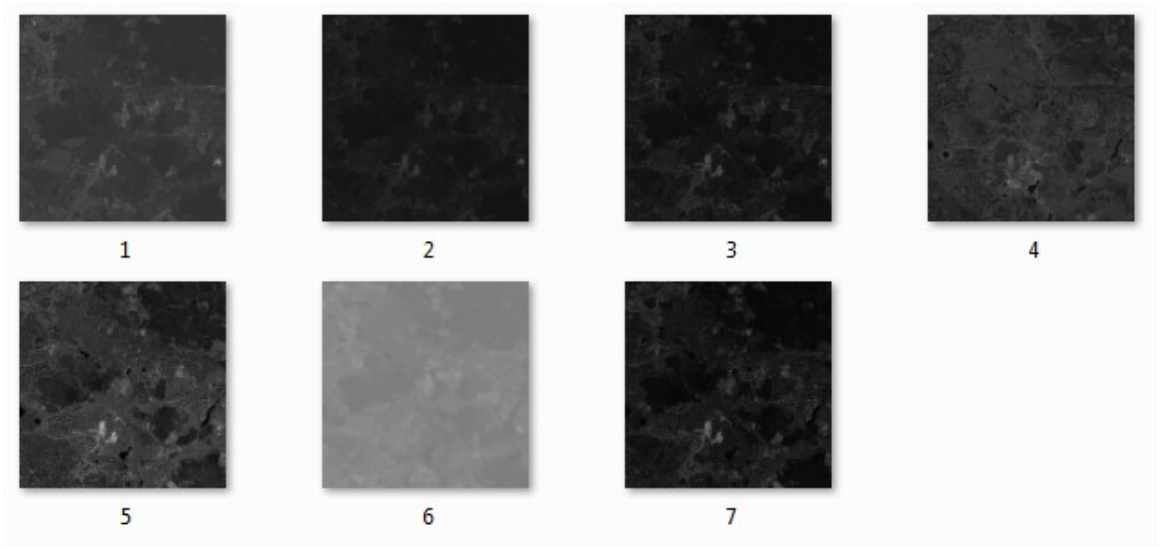

(a)

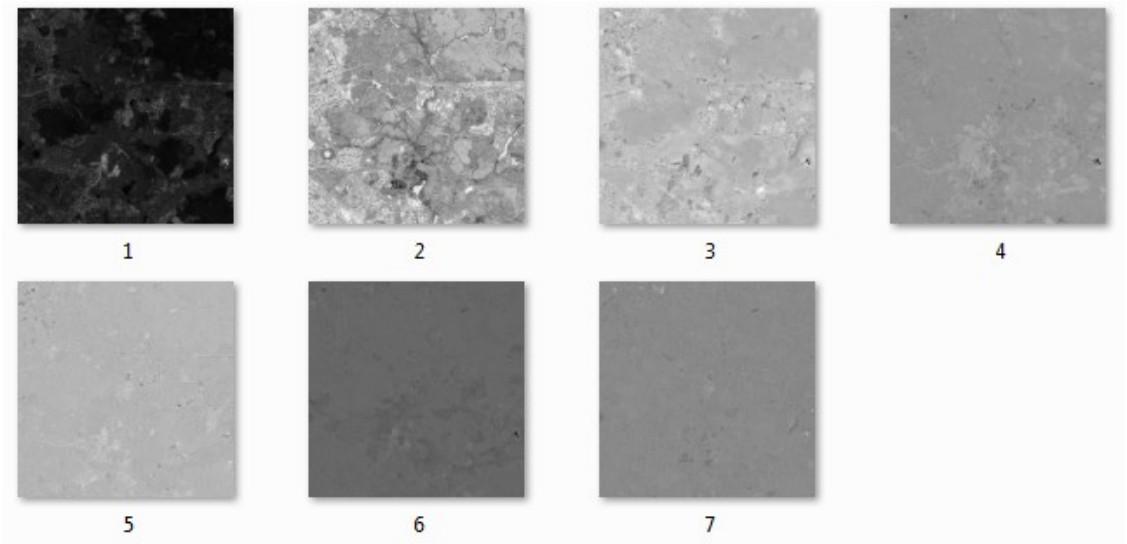

(b)

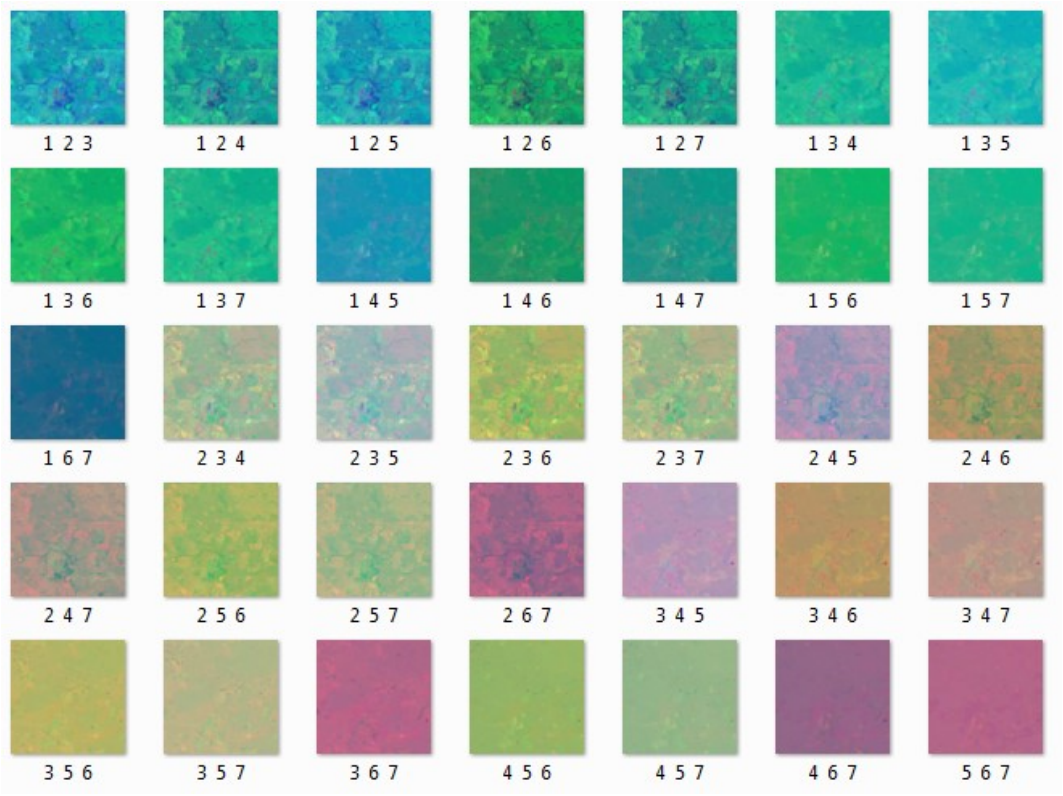

(c)

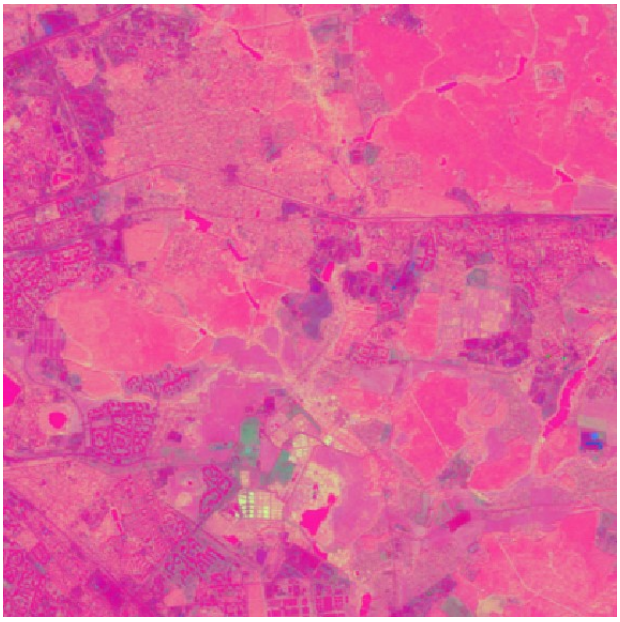

(d)

Fig. 4. Application of the principal component method in the problem of recognizing areas of debris: a) the original image X (canals X^l); b) main components Y^{ll}; c) combination of the main components; d) the best combination ([1 2 6] canals). The transformation operator v is calculated for each image X, i. e. there is no "universal" transformation. In the output composite images, the color of the litter selection may be different, but it differs from the background

The transformation operator v is calculated for each image X, i. e. there is no "universal" transformation. In the output composite images, the color of the litter selection may be different, but it differs from the background.

Fibonacci transformation

The Fibonacci transformation in matrix form can be written as (43):

$$Y = FX, \quad X = F^{-1}Y \tag{43},$$

where X and Y — are matrices of a halftone image of size $n \times n$ in brightness and frequency space; F and F^{-1} — are linear operators of size $n \times n$ of the forward and reverse Fibonacci transformations for the corresponding images X and Y.

The matrix X is obtained by changing the size of the original matrix X with $m \times m$ before $n \times n$, where $n = 2^N$, $N = 1, 2\ldots$, that is, a change in spatial resolution. To do this, the functional is interpolated $z = X(x,y)$, set by a grid of values $x = 1\ldots m$, $y = 1\ldots m$ with a step $h = 1$ (m values along the abscissa and ordinate axes), in the functional $z = X(x,y)$, set by a grid of values $x = 1\ldots m$, $y = 1\ldots m$ with a step $h = (m-1) / n$ (n values along the abscissa and ordinate axes).

The compression of the Y matrix is provided by the compression matrix (selection matrix) (44):

$$S = I_n \otimes s, \quad s = \left\lfloor J_{1*n'} \quad O_{1*(n-n')} \right\rfloor \tag{44},$$

where O_{n*m} — a matrix of size zeros $n \times m$, $n' = n / K$, where $K = 2^{N'}$ — compression ratio of a two-dimensional signal, $N' < N$, $N' = 1, 2\ldots$

The effect of the operator S on Y, acting as a low-pass filter (from 1 to n'), leads to another direct conversion result: $Y' = SFX$. As a result of the reverse conversion F'^{-1} matrix Y' signal $X' = F'^{-1} Y'$ is restored with precision (45):

$$\varepsilon_1 = \rho_{l2}(X, X') = \sqrt{\frac{1}{n^2} \sum_{i=1}^{n} \sum_{j=1}^{n} (x_{ij} - x'_{ij})^2} \tag{45},$$

where l_2 — the standard deviation of the difference matrix $D = X - X'$, $X = [x_{ij}]_{n*n}$; $X' = [x'_{ij}]_{n*n}$, ε_1 — error in restoring a two-dimensional signal as a result of DOT.

Let's evaluate the recovery errors ε_1, ε'_1 for Fibonacci conversion at different compression ratios $j = N'$ and on different channels i of the original image X of the littering area (Kuchino landfill, August 2011). We believe $N = 10$, $\alpha = 10^{-4}$.

Discussion of the results of the Fibonacci transformation

Fig. 5 shows the matrices $E_1 = [\varepsilon_1(i,j)]$, $E_2 = [\varepsilon_2(i,j)]$, $E'_1 = [\varepsilon'_1(i,j)]$, $E'_2 = [\varepsilon'_2(i,j)]$, of sizes $l \times (N - 1)$. We see that the maximum accuracy is observed on the 6-*th* (thermal) channel and it changes slightly during compression. Matrices $E_1 \approx E'_1$.

Fig. 6 shows an example of signal recovery at $N' = N / 2 = 5$. It can be seen from Fig. 6e that an increase in spatial resolution and a decrease in the compression ratio have little effect on the recovery result. In other words, the image of littering can be restored both while maintaining and even reducing the spatial resolution, and with its strong compression. This is due to the fact that the littering texture is characterized by a random, random spatial distribution of pixel brightness.

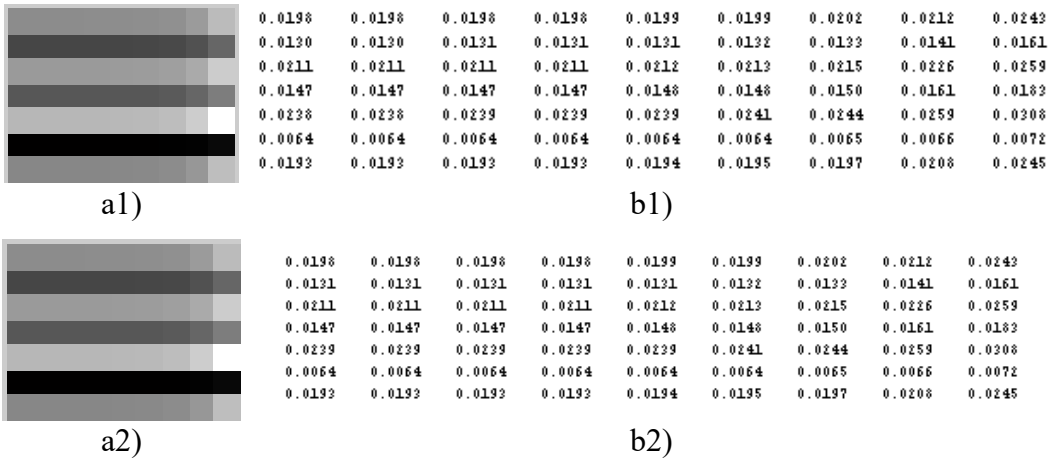

Fig. 5. Recovery errors: 1) ε1; 2) ε'1; a) on different channels and at different compression ratios; b) matrices

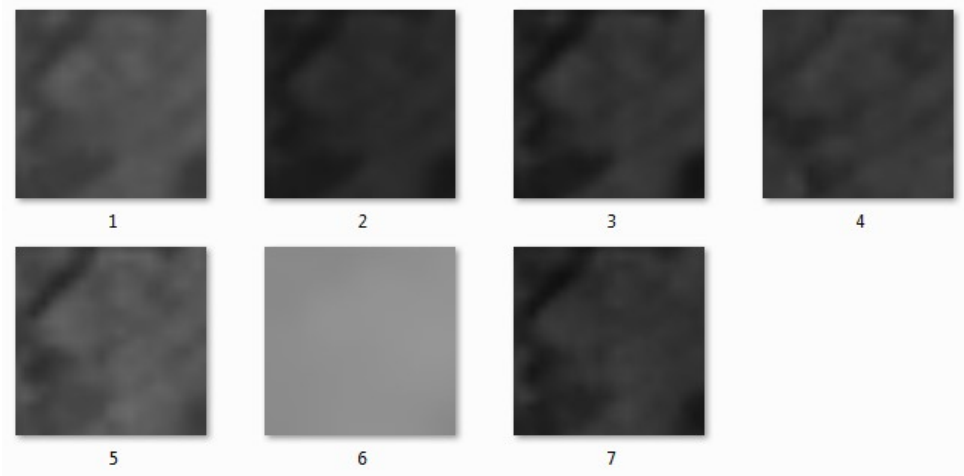

a)

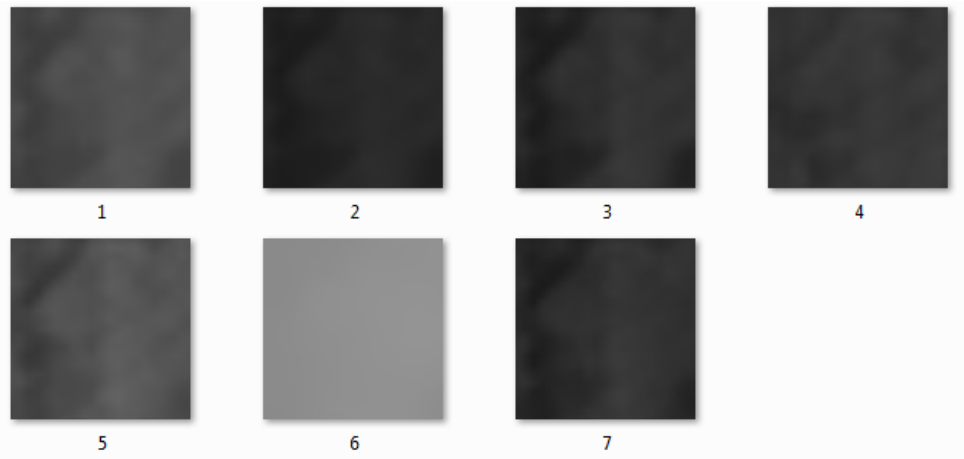

b)

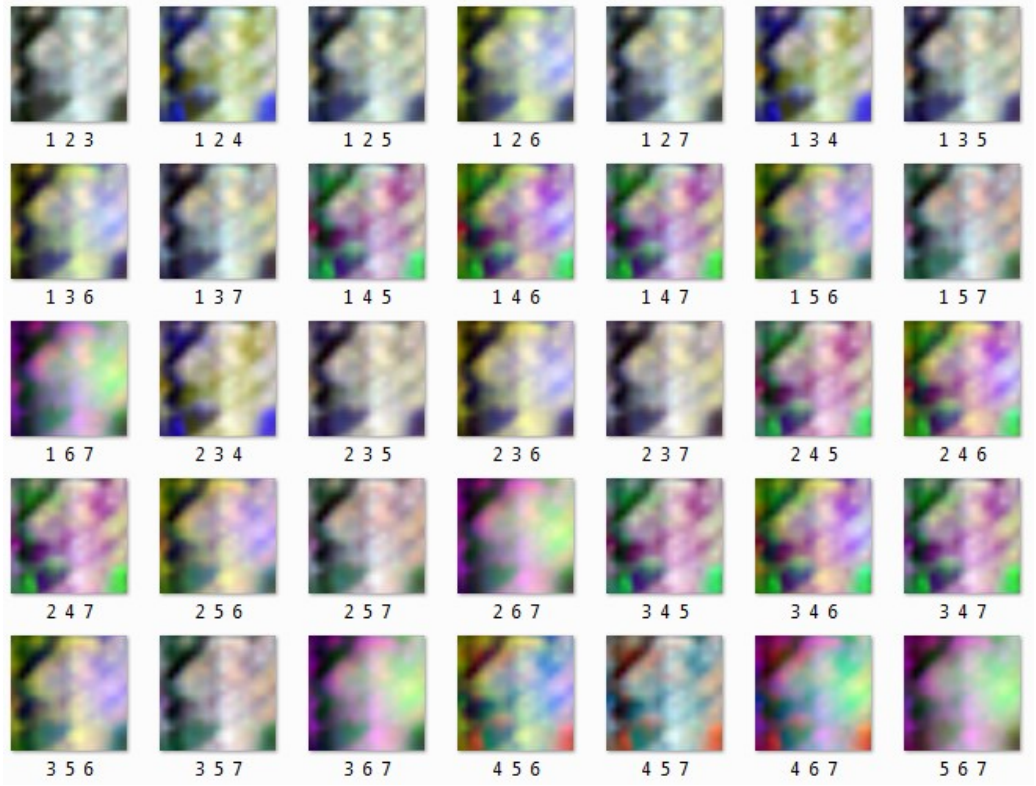
1 2 3
1 2 4
1 2 5
1 2 6
1 2 7
1 3 4
1 3 5
1 3 6
1 3 7
1 4 5
1 4 6
1 4 7
1 5 6
1 5 7
1 6 7
2 3 4
2 3 5
2 3 6
2 3 7
2 4 5
2 4 6
2 4 7
2 5 6
2 5 7
2 6 7
3 4 5
3 4 6
3 4 7
3 5 6
3 5 7
3 6 7
4 5 6
4 5 7
4 6 7
5 6 7

c)

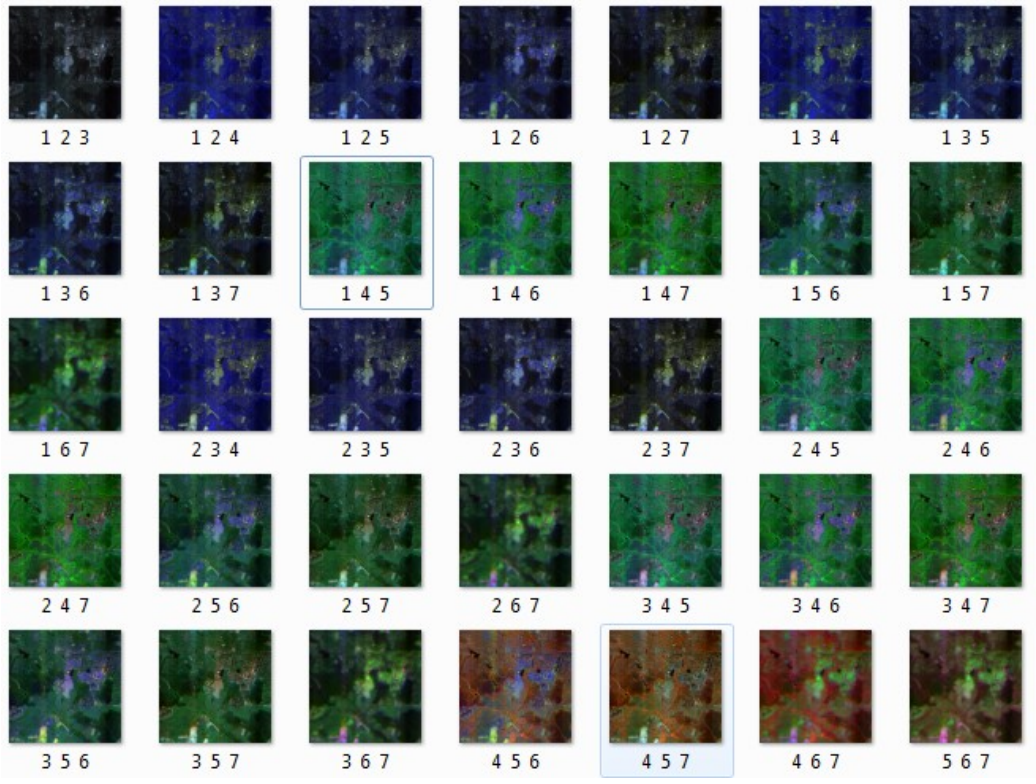
1 2 3
1 2 4
1 2 5
1 2 6
1 2 7
1 3 4
1 3 5
1 3 6
1 3 7
1 4 5
1 4 6
1 4 7
1 5 6
1 5 7
1 6 7
2 3 4
2 3 5
2 3 6
2 3 7
2 4 5
2 4 6
2 4 7
2 5 6
2 5 7
2 6 7
3 4 5
3 4 6
3 4 7
3 5 6
3 5 7
3 6 7
4 5 6
4 5 7
4 6 7
5 6 7

d)

e1)

e2)

Fig. 6. An example of the Fibonacci transformation of a littering image:
a) the original images (with an increase in spatial resolution, N = 10);
b) the Fibonacci transformation with compression (N′ = 5);
c) the composites of transformations (combining different channels, N = 8, N′ = 2);
d) the best transformation (combination [3 5 7]);
e) examples of images (1 — N = 8, N′ = 2; 2 — N = 10, N′ = 3)

CONCLUSIONS

The paper provides a detailed mathematical study of Fibonacci transformations. A statement related to the Karunen-Loew transformation and a theorem are proved, in which the type of the selection matrix *S* is specified when performing compression by means of zone coding using a discrete Fibonacci transformation.

An experiment is being conducted, which is carried out in two stages. The first stage is the application of a DOT onto the original image to perform image decorrelation and decrease the dimension of the original image accordingly. The second stage consists in the formation of a trained classifier for decrypting the image.

These studies find application in conducting space monitoring of the Earth using a remote sensing device to prevent environmental and emergency situations on a global scale.

REFERENCES

Agaian S. S. Successes and problems of fast orthogonal transformations. Recognition, classification, prognosis. Moscow: Nauka, 1990. Iss. 3. P. 146–214 (in Russian).

Agaian S. S., Aizenberg N. N., Alaverdian S. B. Discrete Fibonacci transformation. Problems of theoretical cybernetics. Abstracts of the III World Conference. Gorky, 1988. P. 5–67 (in Russian).

Agaian S., Alaverdian S. Fast orthogonal Fibonacci transform. Osaka, Japan: Proc. Int. Coll. On Coding Theory, 1998. P. 335–353.

Bergman G. A number system with an irrational base. Mathematics Magazine, 1957. No. 31. P. 98–119.

Bertrand-Mathis A. Comment écrire les nombres entiers, dans une base qui n'est pas entière. Acta Mathematica Hungarica, 1989. V. 54. No. 3–4. P. 237–241 (in French).

Chernov V. M. Discrete orthogonal transformations on fundamental domains of canonical number systems. Computer optics, 2013. V. 37. No. 4. P. 484–488 (in Russian).

Chernov V. M. Discretionary orthogonal transformations at the molecular level associated with complete researchers. Proceedings of the Institute of Mathematics and Mechanics of the Russian Academy of Sciences, 2020. V. 26. No. 3. P. 249–257 (in Russian).

Crippen R. E. Calculating the vegetation index faster. Remote Sensing of Environment, 1990. V. 34. P. 71–73.

Fraenkel A. Systems of numeration. American Mathematical Monthly, 1985. V. 92. P. 105–114.

Fraenkel A. The use and usefulness of numeration systems. Information and Computation, 1989. V. 81. No. 1. P. 46–61.

Garcia L. A., Foged N., Cardon G. A GIS-Based Model to Estimate Relative Reductions in Crop Yield Due to Salinity and Waterlogging: Philosophy and Development. ASCE Journal of Irrigation and Drainage Engineering, 2006. No. 132(6). P. 553–563.

Glumov N., Myasnikov V., Sergeyev V. Polynomial bases for image processing in a sliding window. Pattern Recognition and Image Analysis, 1994. V. 4. No. 4. P. 408–413.

Golubov B. I., Efimov A. V., Skvortsov V. A. Walsh series and transformations: Theory and applications. Moscow: URSS, LKI, 2008. 352 p. (in Russian).

Gonzalez R., Woods R. Digital image processing. Moscow: Technosphere, 2019. 1104 p. (in Russian).

Gradstein I. S., Ryzhik I. M., Tables of integrals, sums, series and products. Moscow: Fizmatgiz, 1963. 1100 p. (in Russian).

Hall M. Combinatorial Theory. Waltham (Massachusetts)–Toronto–London: Blaisdell Publishing Company, 1967.

Ivashko A. V., Algorithms and devices for digital processing and data transmission based on integer exponential basis sequences. Abstract of the dissertation… of PhD of technical sciences. Kharkov, 1983. 20 p. (in Russian).

Kazaryan M. L. Mathematic — systemic researching with the involvement of fractals when processing of space surveillance systems on recognition of waste disposal objects. Aerospace Research in Bulgaria. Bulgarian Academy of Sciences. Space Research and Technology Institute, 2021. V. 33. P. 124–139.

Kazaryan M. L., Shakhramanyan M. A., Nedkov R., Borisova D., Avetisyan D. Fractal presentation of space images during waste disposal sites monitoring. Proceedings of Seventh International Conference on Remote Sensing and Geoinformation of the Environment (RSCy2019), 2019 (a). V. 111740. DOI: 10.1117/12.2532890.

Kazaryan M. L., Shahramanian M. A., Voronin V. V. The automated space-monitoring system of waste disposal sites. Remote Sensing Technologies and Applications in Urban Environments III, Berlin, Germany: Proceedings of SPIE Remote Sensing, 2018 (a). V. 1079318. DOI: 10.1117/12.2500059.

Kazaryan M. L., Shahramanian M. A., Zabunov S. Investigation of the similarity algorithm of the satellite images storage system for stability on the basis of Haar wavelets according to Tikhonov. Aerospace Research in Bulgaria**,** Bulgarian Academy of Sciences. Space Research and Technology Institute, 2019 (b). V. 31.

Kazaryan M. L., Shahramanian M. A., Zabunov S. Investigation of the basic Haar wavelet-transformations in the problem of decryption of space images on detection of waste disposal fields. Aerospace Research in Bulgaria. Bulgarian Academy of Sciences. Space Research and Technology Institute, 2018 (b). V. 30. P. 96–103.

Kazaryan M. L., Voronin V. V. Satellite image processing based on percolation for physico-chemical analysis of soil cover of industrial waste facilities. Sensors and Systems for Space Applications XIV. Proceedings of SPIE, 2021. V. 117550W. DOI: 10.1117/12.2587769.

Korn G., Korn T. Handbook of Mathematics for researchers and Engineers. Definitions, theorems, formulas. Moscow: Nauka, 1978. 832 p. (in Russian).

Lezhnev A. Dynamic programming in economic problems: A textbook. Moscow: Prosveshchenie–Binom, 2017. 505 p. (in Russian).

Manzo C. Integrated remote sensing for multi-temporal analysis of anthropic activities in the south-east of Mt. Vesuvius National Park. Journal of African Earth Sciences, 2016. V. 122. P. 63–78.

Nadudvari A. Thermal mapping of self-heating zones on coal waste dumps in Upper Silesia (Poland). International Journal of Coal Geology, 2014. V. 128–129. P. 47–54.

*Shovengerdt R. A. R*emote sensing. Models and methods of image processing: A textbook. Moscow: Technosphere, 2013. 624 p. (in Russian).

Stakhov A., Luzhnetsky V. Computer arithmetic of digital computers in Fibonacci codes and the "golden" proportion. Moscow: Academy of Sciences of USSR, 1981. 64 p. (in Russian).

Umnyashkin S. V. Fundamentals of the theory of signal processing: A textbook. Moscow: Technosphere, 2021. 550 p. (in Russian).